Person to person droplets transmission characteristics in unidirectional ventilated protective isolation room: The impact of initial droplet size

Caiqing Yang[12], Xudong Yang[1] (✉), Bin Zhao[1]

1. Beijing Key Laboratory of Indoor Air Quality Evaluation and Control, Department of Building Science, Tsinghua University, Beijing 100084, China
2. Beijing Institute of Architectural Design, Beijing 100045, China

Abstract

Person to person droplets/particles or contaminant cross transmission is an important issue in ventilated environment, especially in the unidirectional ventilated protective isolation room (UVPIR) where the patient's immune system is extremely low and easily infected. We simulated the dispersion process of the droplets with initial diameter of 100 μm, 10 μm and gaseous contaminant in unidirectional ventilated protective isolation room and studied the droplets dispersion and cross transmission with different sizes. The droplets with initial size of 100 μm settle out of the coughing jet quickly after coming out from mouth and cannot be carried by the coughing jet to the human thermal plume affecting (HTPA) zone of the susceptible manikin. Hence, the larger droplets disperse mainly in the HTPA zone of the source manikin, and the droplets cross transmission between source manikin and susceptible manikin is very small. The droplets with initial size of 10 μm and gaseous contaminant have similar dispersion but different removal process in the UVPIR. Part of the droplets with initial size of 10 μm and gaseous contaminant that are carried by the higher velocity coughing airflow can enter the HTPA zone of the susceptible manikin and disperse around it. The other part cannot spread to the susceptible manikin's HTPA zone and mainly spread in the source manikin's HTPA zone. The results from this study would be useful for UVPIR usage and operation in order to minimize the risk of cross infection.

1 Introduction

Transmission of infectious diseases in indoor environment has been receiving more and more attentions. Existing research shows that some infectious diseases such as SARS, tuberculosis, influenza, etc. can all spread through air (Yu et al. 2004; Li et al. 2007). Humans produce droplets during expiratory activities such as coughing, talking, and sneezing. If these droplets are produced by an infected person, pathogenic contaminants can be transmitted to other people and lead to cross-infection.

Single room isolation with unidirectional, high efficiency particulate air filter (HEPA) filtering airflow from the entire ceiling unit has been used to protect patients who need the most protection (Yang et al. 2015). In such clean wards, "laminar" (not in real sense) airflow moves in parallel and same direction with almost same velocity from the air supply

opening to the air return opening (Gregory et al. 2007). Such a unidirectional airflow ventilation system is believed to be able to control the particle/droplet or other contaminant cross transmission and can be removed effectively. Some existing study indicated that unidirectional ventilation system combined with an appropriate air filtration system could greatly decrease the cross infection risk and increase patient survival rate effectively (Storb et al. 1983; Barnes and Rogers 1989; Passweg et al. 1998; Schlesinger et al. 2009).

As discussed in previous study, although the unidirectional ventilated protective isolation room (UVPIR) is patient room in hospital, it has difference with airborne infection isolation room (AIIR) and operating theatre (OT) (Yang et al. 2015). Hence, the research findings in AIIR and OT may not applicable in UVPIR. Laminar airflow system has been widely used in operating theatre to decrease rates of surgical site infections (SSI). In recent years, some scholars

E-mail: xyang@tsinghua.edu.cn

doubted the effect of laminar airflow on the reduction of wound infections. For example, Gastmeir et al. (2012) investigated the influence of laminar airflow on the surgical site infections and concluded that it would be a waste of resources to establish new operating room with laminar airflow system. James et al. (2015) reviewed the current literature for the use of laminar airflow operating theatre ventilation during total joint arthroplasty and examined the effectiveness of laminar airflow on preventing post-operative wound infection and found that there is no conclusive effect on the reduction of post-operative wound infections by laminar airflow system. The vertical laminar airflow system directs air from ceiling to floor. The airflow passes over the head and upper body of the surgeon and assistants to the surgical site. During surgical procedures, bacteria-laden dust particles, textile fibers, and respiratory aerosols may be released from the surgical team in to the air of the operating room. These bacteria may be carried by the downward airflow to settle on the surgical instruments or directly enter the surgical site and lead to surgical site infection (James et al. 2015; McHugh et al. 2015). The key reason that the vertical laminar airflow may lead to surgical site infection is that the bacteria sources (the head and upper body of the surgeon and assistant) located at the upper area of the patient. The relative positions of patient and doctors or nurses are different in UVPIR and operating theatre. The vertical laminar airflow from the whole ceiling in the UVPIR will create an entire protective environment for the patient from being infected from doctors or nurses who may enter into the ward. The bacteria from the doctors or nurses will be carried by the downward airflow to the floor level and removed from the exhaust opening located at the bottom of the two sidewalls. Hence, using vertical laminar airflow system to decrease cross infection risk is more appropriate in UVPIR than in operating theatre.

A lot of related work on person to person droplets/particles or contaminant cross transmission in different ventilation systems can be found in the literature. For example, Chen et al. (2010) investigated the droplets/particles cross transmission between dental healthcare workers and patient. Cao et al. (2015) examined the performance of protected zone ventilation and hybrid protected zone ventilation in reducing person to person airborne cross transmission in office room by experiment. Habchi et al. (2014) studied the cross-infection between occupants in the room with a mathematical multi-plume multi-layer transport model. Habchi et al. (2016) investigated the direct and indirect cross-contamination in office space with ceiling personalized ventilation combined with desk fans. He et al. (2011) investigated the exhaled droplet cross-transmission between occupants in a typical office room with different ventilation strategies. Li et al. (2011) adopted a novel modeling approach to directly assess the inhalation dose of infectious droplets and estimated the exposure risk for the co-occupant under different ventilation methods. Olmedo et al. (2013) investigated the risk of airborne cross-infection between the two breathing thermal manikins in a room with vertical low-velocity ventilation. Nielsen et al. (2012) studied the cross transmission of the exhaled small particles between two people standing in surrounding with a vertical temperature gradient. Most of these studies indicated the importance of using appropriate particle sizes in conducting this type of study. The issue is particularly important for UVPIR where the patient may be exposed to various types of bio-aerosols generated from others.

Back in the 1940s, Duguid (1946) studied the sizes of droplets from speaking, coughing and sneezing through microscopic measurement, and found that the range of the droplets diameters was from 1 μm to 2000 μm and 95% of the droplets were less than 100 μm. Chao et al. (2009) measured the droplet size using the interferometric Mie imaging (IMI) technique. The droplet size distribution obtained by their study was more in line with the data obtained by Duguid (1946). The geometric mean diameter of the droplets expelled from coughing and speaking was 13.5 μm and 16.0 μm, respectively from their study. The droplet concentrations were range from 0.004 to 0.223 cm^{-3} for speaking and 2.4–5.2 cm^{-3} per cough for coughing. The average number of droplets/particles emitted each sneeze and cough was 1×10^6 and 5×10^3, respectively. Larger droplets may settle out of the airflow quickly and thus the cross transmission only happens when the individuals are close enough. Smaller droplets may hang in the air for longer time and spread for longer distance, thus will have higher risk of cross transmission between person to person (Riley 1974; Brachman 1990). Overall, existing research showed that the droplets of different sizes have different dispersion characteristics and cross transmission risk.

Previously, we have developed a computational model to simulate the airflow and contaminant dispersion in UVPIR (Yang et al. 2015). However, air contaminant generated from human source was overly simplified as gaseous in that study. The goal of this study is to further understand the droplets dispersion characteristics and cross transmission risk with different sizes in unidirectional ventilated protective isolation room.

2   Research methods

2.1   Mathematic model

In our previous study, CFD software (Fluent 2005) was used to simulate the airflow and gaseous contaminant concentration in UVPIR. RNG k–ε turbulence model was selected to

simulate the airflow field in UVPIR. The simulation model was validated against experimental data (Yang et al. 2015). Built upon this airflow model, we intend to simulate the dispersion process of the droplets with the following three initial sizes: large (100 μm), medium (10 μm), and small (represented by gaseous contaminant). Particles smaller than 2 μm were found to share the common dispersion and transport properties of air (Chen et al. 2006). It is feasible to simulate the smaller particle with species transport model, but not for larger particles concerned in this study.

Each droplet released from manikin's mouth was tracked individually in a Lagrangian frame for its instantaneous position, velocity and other parameters. Generally for the particles observed in indoor air, other forces such as the Basset history, the pressure gradient and the virtual mass are negligible compared with the drag force (Zhao et al. 2004). The density and size of the droplets investigated in this study are all similar with their study, hence, the Basset force, the pressure gradient force and the virtual mass force are ignored in our simulation. The Stokes drag force, the Saffman's lift force, thermophoretic force and gravitational force were considered in this study. Thus, the Lagrangian equations describing the motion of the droplets are

$$\frac{dx_p}{dt} = u_p \tag{1}$$

$$\frac{du_p}{dt} = \frac{f_D}{\tau_p}(u - u_p) + F_p \tag{2}$$

where x_p is the move distance, t is the time, u_p is the velocity of the droplet. F_p represents other external forces; Saffman's lift force, thermophoretic force and gravitational force are considered in this study. f_D is the Stokes drag modification function. For large droplet Reynolds number (Re_p), f_D is defined as (Clif et al. 1978)

$$f_D(Re_p) = 1 + 0.15Re_p^{0.687} \tag{3}$$

The droplet characteristic time in Eq. (2) is defined as

$$\tau_p = \frac{\rho_p D_p^2 C_c}{18\mu} \tag{4}$$

The Cunningham slip correction factor C_c for small size droplets in Eq. (4) is

$$C_c = 1 + \frac{2\lambda}{D_p}\left(1.257 + 0.4\exp\left(-\frac{1.1D_p}{2\lambda}\right)\right) \tag{5}$$

ρ_p is the density of the droplet, D_p is the diameter of the droplet, λ is the mean free path.

The gradient of diffusion due to the vapor pressure equilibrium at the droplet's surface is used to calculate the vaporization rate of the droplets:

$$\frac{dN}{dt} = c(C_s - C_\infty) \tag{6}$$

$$Nu_{AW} = \frac{cD_p}{D_m} = 2.0 + 0.6Re_p^{0.5}Sc^{\frac{1}{3}} \tag{7}$$

$$C_s = \frac{p_{sat}(T_p)}{RT_p} \tag{8}$$

$$C_\infty = X_i \frac{p_{op}}{RT_\infty} \tag{9}$$

where Nu_{aw} is the Nusselt correlation at the air–water interface. D_m is the mass diffusion coefficient. c in Eqs. (6) and (7) is the mass transfer coefficient; the value of c is calculated from a Nusselt correlation (Ranz and Marshall 1952). Sc is the Schmidt number. R is the universal gas constant. $p_{sat}(T_p)$ is the saturated water vapor pressure. T_p is the temperature of the droplets. X_i is the local bulk mole fraction of water vapor, p_{op} is the operating pressure, and T_∞ is the local bulk temperature in the air.

Heat balance equation is used to simulate the droplet temperature. It is the sensible heat change in the droplet to the latent heat of evaporation and the convective heat transfer between the droplet and the air:

$$m_p C_p \frac{dT_p}{dt} = \frac{dm_p}{dt}H_{fg} + \pi H d_p^2(T - T_p) \tag{10}$$

where m_p is the mass of droplet, C_p is the specific heat capacity of droplet, H_{fg} is the latent heat of evaporation. H is the heat transfer coefficient, and is obtained in similar way:

$$Nu = \frac{HD_p}{\kappa_{eff}} = 2.0 + 0.6Re_p^{0.5}Pr^{\frac{1}{3}} \tag{11}$$

where κ_{eff} is the effective thermal conductivity, Pr is Prandtl Number.

2.2 Validation of the droplets simulation model

The airflow turbulence model and gaseous contaminant simulation model have been validated previously (Yang et al. 2015). We only need to validate the droplet simulation model here.

Chao and Wan (2006) tested the dispersion of expiratory aerosols in unidirectional downward ventilation room with dimensions of 4.8 m × 4.8 m × 2.6 m (width × length × height). The tested ventilation type is quite similar to unidirectional ventilated protective isolation room investigated in this study. The droplet emission source was located at the center of the testing room, 0.8 m above the floor. Droplets were emitted vertically upward. We simulated their experimental cases with the simulation model discussed above and compared with the data. Figure 1 indicates that the predicted
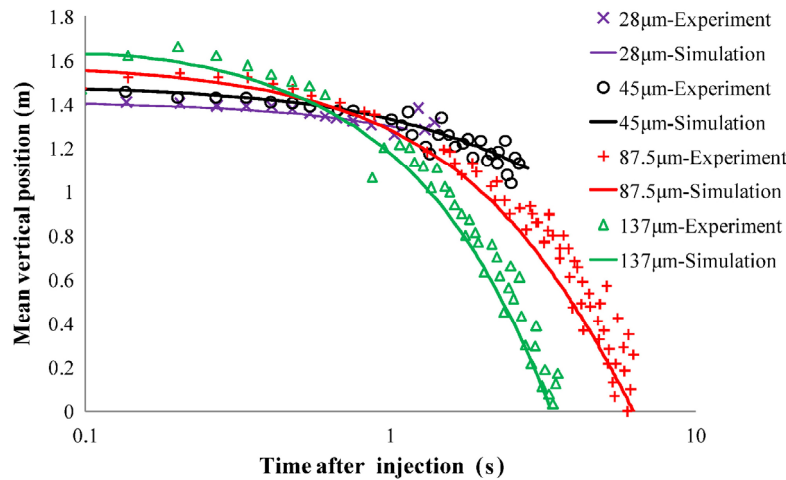
Fig. 1 The comparison of the predicted vertical position of the droplets with the experimental data by Chao and Wan (2006)

vertical position trajectory of droplets matches well with the experiment results.

2.3   The description of the investigated scenario

We simulated the droplets cross transmission between two manikins in UVPIR in this study. The size of the room is 3 m × 2.5 m × 3 m (width-X, height-Y, and length-Z). Clean air is supplied into the room through ceiling-mounted HEPA filters with the opening size of 3 m × 3 m (width-X and length-Z). The air is exhausted from the outlets located on the bottom of two sidewalls of the room, with each opening size being 0.3 m × 3 m (height-Y, and width-X). Two standing manikins with 1.0 m apart are located in the room, as shown in Fig. 2. The blue manikin represents the susceptible and the red manikin represents the source. The heights of both manikins are 1.7 m.

Wells (1934) defined large droplets as those over 100 μm in aerodynamic diameter. Hence, 100 μm is selected in this study to investigate the transmission characteristics of large

Fig. 2 The schematic of the simulated room and manikins

droplets. Lindsley et al. (2010) measured the influenza virus in aerosol particles from human coughs and found that not only that coughing by patients emitted aerosols containing the influenza virus, but also that much of the influenza viral was contained within particles in the respirable size range. 35% of the detected influenza RNA was contained in particles >4 μm, 23% in particles of 1–4 μm, and 42% in particles <1 μm. 10 μm is selected in this study to examine the transmission characteristics of medium droplets. Gaseous contaminant is also studied to represent small droplets (smaller than 1 μm) and chemical contaminant.

2.4   Boundary conditions

Velocity inlet boundary condition was used for the inlet opening, the supply air velocity was 0.25 m/s which was recommended by Yang et al. (2015) and the supply air temperature was set to 24 °C. The mass flow rate at outlet was equal to that of inlet. The heat fluxes of room enclosure surfaces were all set to 0. The body surface temperature of the manikins was set to 33 °C (Yang et al. 2015). Based on the research of McFadden et al. (1985), the temperature of coughing air from source manikin's mouth and the breathing air from both source and susceptible manikins' noses were set to 32 °C.

The flow boundary conditions at the mouth and nose of the source manikin were different depending on whether he/she was breathing or coughing. In our simulation, the coughing airflow came from source manikin's mouth; the airflow from source manikin's nose was 0 during coughing. After coughing, the source manikin breathed with nose and the airflow rate from mouth was 0. The susceptible manikin breathed with nose during all simulating time and the airflow rate from his/her mouth was 0. The boundary conditions of the exhalation at source manikin and susceptible manikin's
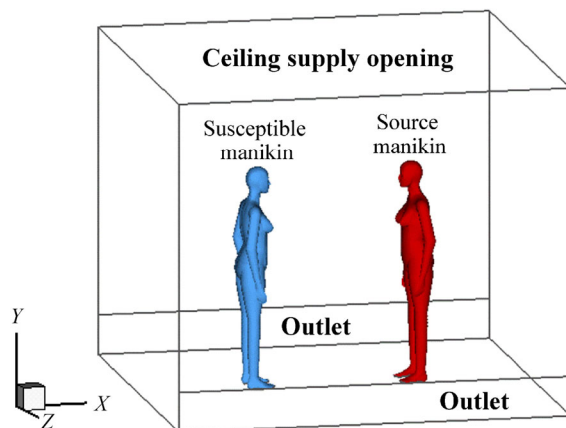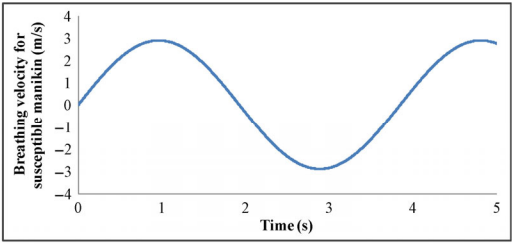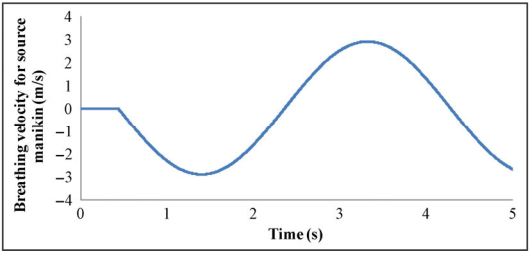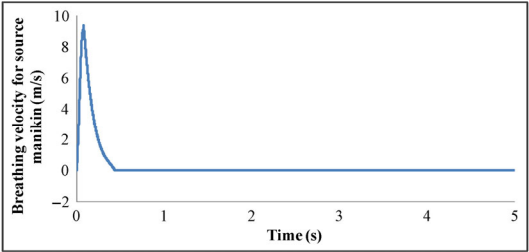
mouth and nose were specified according to the study of Gupta et al. (2009, 2010). Droplets were composed of organic ions, aqueous solution containing inorganic and glycoproteins.

The relative humidity has great influence on the dispersion of the droplets in the room. Low relative humidity results in rapid evaporation and thus leads to the increase of the suspended particles in the room air (Arundel et al. 1986).

The relative humidity (RH) in the supply air was set to 50%, as recommended by the Chinese standard GB 50457-2008 (2009). The relative humidity of the breathing and coughing air was set to 100%. When expelled from source manikin's mouth, the droplets entered into an environment that had a lower temperature and relative humidity than that in the coughing air. The detailed settings of boundary conditions are shown in Table 1.

Table 1 The boundary conditions in the simulation

Boundary	Physical parameter		Value
Supply airflow	Velocity		0.25 m/s
	Temperature		24 °C
	Relative humidity		50%
Breathing airflow from susceptible manikin	Velocity	Nose	
		Mouth	0
	Temperature		32 °C
	Relative humidity		100%
Coughing jet and breathing airflow from source manikin	Velocity	Nose	
		Mouth	
	Temperature		32 °C
	Relative humidity		100%
Human body surface	Temperature		32 °C
Droplets	Inlet		Reflect
	Outlet		Escape
	Nose/mouth		Escape
	Human body surface and walls		Trap
Droplet material characteristics	Material		Water
	Initial temperature		32 °C
	Volatile fraction		98.2%
	Binary diffusivity		0.288 cm^2/s

3   Results and discussion

The airflow field in the simulated UVPIR is shown in Fig. 3. The stream lines are almost parallel above the manikins' heads. The downward airflow directions are changed by the thermal plume from manikin and created two "human thermal plume affecting zones" (HTPA zones), which is defined as the vortex area affected by the human thermal plume (Yang et al. 2014). The downward airflow near the manikin is pulled up by the manikin thermal plume and creates a vortex airflow around the human body. The existence of the HTPA zone has mixed effects. On one hand, the HTPA zone around the manikin can create a protective barrier and prevent the contaminant from entering the zone
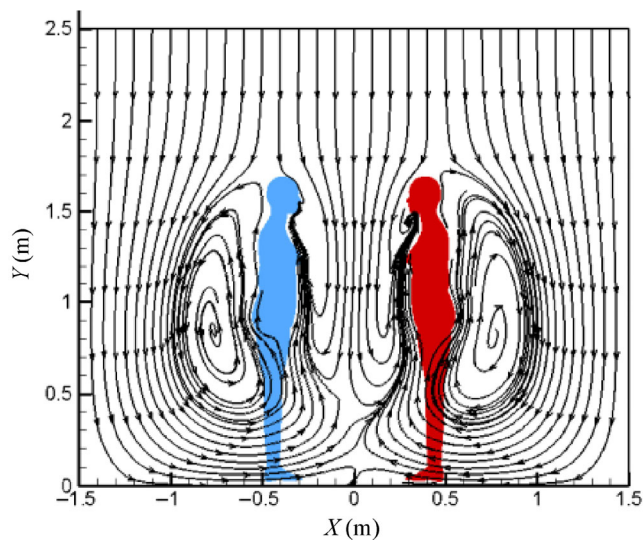
and avoid contaminant cross transmission. On the other hand, if the contaminants are entrained into the HTPA zone, the upward airflow in the zone will carry the contaminant to the manikin's breathing zone and lead to cross transmission. The effective way to decrease cross transmission is to prevent contaminants from entering the HTPA zone of the susceptible manikin.

The dispersion process of the droplets with initial diameter of 100 μm from coughing is shown in Fig. 4. These droplets carried by the coughing jet can move forward for a very short distance (less than 0.3 m) before going downward, and mainly disperse in the HTPA zone of the source manikin after that. The droplets settle out of the coughing jet quickly after emitted from source manikin's mouth. Very few droplets remain in the UVPIR one minute after.

Figure 5 shows the dispersion process of the droplets with initial diameter of 10 μm. Approximate 60% of the droplets carried by the coughing jet move forward for approximately 0.6 m, enter into and disperse in the HTPA zone of the susceptible manikin. The other parts of droplets (approximate 40%) remain in the HTPA zone of the source manikin and mainly disperse around the source manikin area. As shown in Table 1, the peak coughing velocity can reach 9 m/s. Such high velocity coughing jet can easily break out the protective barrier and enter into the HTPA zone of susceptible manikin. However, after coughing, the source manikin respires via nose. The peak breathing velocity drops down to 2.9 m/s. During the respiration process, the breathing air cannot break out the protective barrier and enter the HTPA zone of the susceptible as shown in Fig. 5. Hence, when the velocity of the coughing airflow is higher (much higher than 2.9 m/s), the droplets can be carried by the high
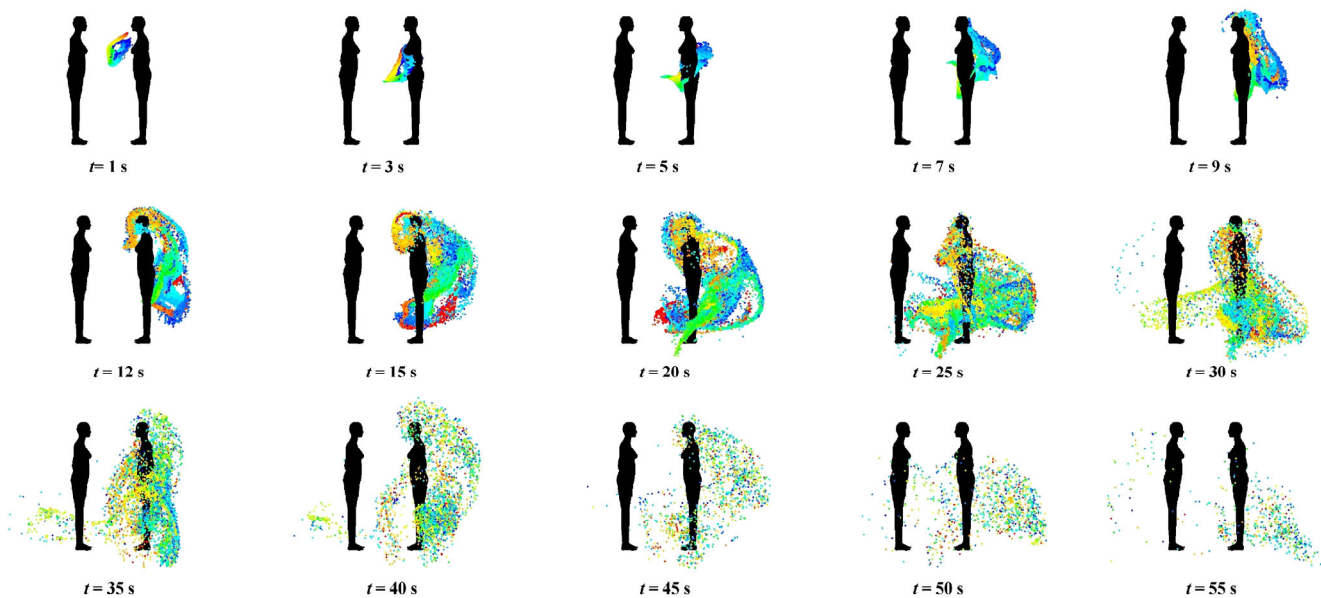

Fig. 3   The airflow field in the UVPIR

Fig. 4   The dispersion process of droplets with initial diameter of 100 μm

velocity coughing jet to the susceptible manikin's HTPA zone. But when the velocity of the coughing airflow is lower, the droplets cannot reach the susceptible manikin's HTPA zone. One minute after, most of the droplets are removed from the room.

The dispersion process of the gaseous droplets is shown in Fig. 6. Similar to the dispersion process of the droplets with initial diameter of 10 μm, part of the gaseous contaminants are carried by the higher velocity coughing jet to a longer

distance in 3 seconds and enter the HTPA zone of the susceptible manikin directly. Other gaseous contaminants carried by the lower velocity coughing airflow remain in the HTPA zone of the source manikin. Five seconds after, the two parts of gaseous contaminants are dispersed in the HTPA zones of susceptible and source manikins respectively. The gaseous contaminant concentrations in the area close to the body of two manikins are higher than that of other places. The contaminant is diluted gradually with time.
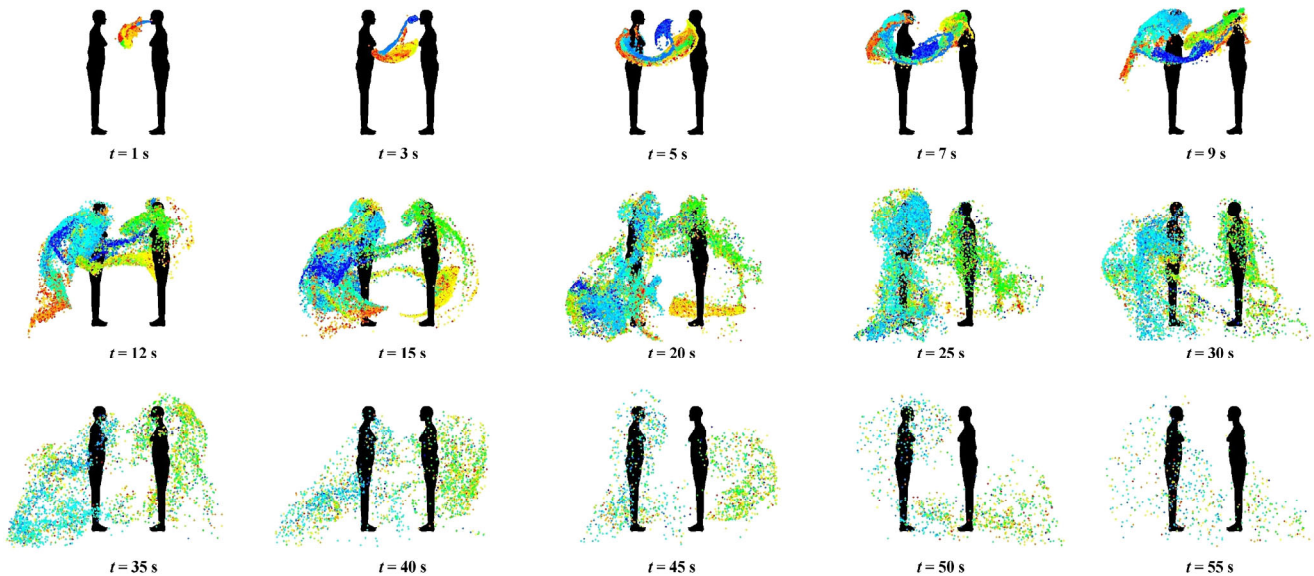

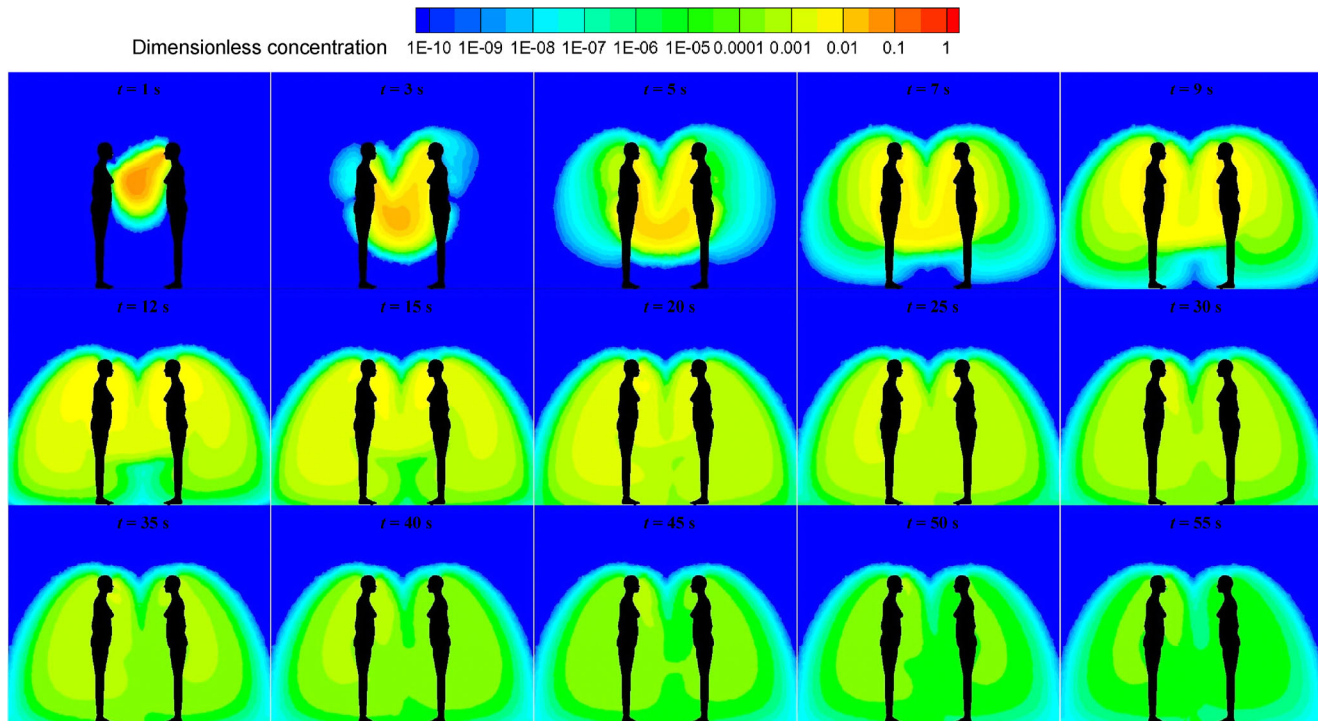Fig. 5 The dispersion process of droplets with initial diameter of 10 μm

Fig. 6 The dispersion process of gaseous droplets

One minute after, the contaminant concentration near the manikin is already diluted by 10 000 times.

The dispersion processes of the droplets with initial diameter of 10 μm and gaseous contaminant are similar from the comparison between Figs. 5 and 6. Figure 7 shows how the droplet sizes change with time for different initial size droplets. For the droplets with initial size of 10 μm, the size remains nearly the same in the first 2 seconds due to high relative humidity of the breathing air, and then decreases rapidly to 2.6 μm in the following 0.4 seconds. The droplets with initial size of 10 μm become droplet nuclei with size of 2.6 μm rapidly after entering into the room. Zhao and Wu (2005) proposed an indicator to judge whether the particle can be treated as passive transport or gaseous contaminant. By calculating, we found when the particle size is less than 10 μm, the indicators of the droplets/particles in UVPIR under 0.25 m/s air supply velocity are all lower than the upper limit (2.8E−02 s^2) suggested by Zhao and Wu (2005). Based on this, if the size of the droplet nuclei is less than 10 μm (which corresponds to 30 μm initial size of the droplet from Fig. 7), the droplet dispersion would be similar to that of gaseous contaminant. The droplets with initial size of 100 μm need 6 seconds to become the droplets nuclei with the size of 26 μm. For larger particles, the dispersion characteristics are of great difference than gaseous contaminant.

Figure 8 shows the total quantity of droplets changing with time in the UVPIR. For the droplets with initial size of 100 μm and 10 μm, only 1% left in the room air after one minute. But for the gaseous contaminant, 15% of the contaminant left in the room air after one minute. Although the droplets with initial size of 10 μm and the gaseous contaminant have similar dispersion process in the UVPIR, their total quantities in the room air decay process are different. The reason is that the droplets deposit on the surfaces in the room during the transmission, not the gaseous contaminant. The quantity of the droplets with initial size of 100 μm has a rapid decrease in the first 5 seconds. The reason is that the droplets mainly disperse around the source manikin body surface in the first 10 seconds (as shown in Fig. 4), which leads to a great chance of settling and over 10% of the droplets deposit onto the body surface. The quantity of the droplets with initial size of 10 μm also has obvious decay at the first 15 seconds, but both the amount and the rate of decay are much smaller than that of the droplets with initial size of 100 μm. For the decay process of the gaseous contaminant, the quantity of the gaseous contaminant remains unchanged at the first 10 seconds and decreases gradually after that. The total amount of the gaseous contaminant drops to 20% in 30 seconds, and the decay rate becomes quite small after that. One minute after, 15% of the gaseous contaminant remains in the room.

The schematic diagram of the dispersion process of the droplets in the UVPIR is summarized in Fig. 9. From the discussions above, large droplets have larger settling velocity, so that the droplets settle out of the coughing jet quickly after coming out from mouth and cannot be carried by the coughing jet to the HTPA zone of the susceptible manikin. Hence, the larger droplets disperse mainly in the HTPA zone of the source manikin, and the droplets cross transmission between source manikin and susceptible manikin should be very small. But for small droplets/gaseous contaminants, part of them are carried by the higher velocity coughing
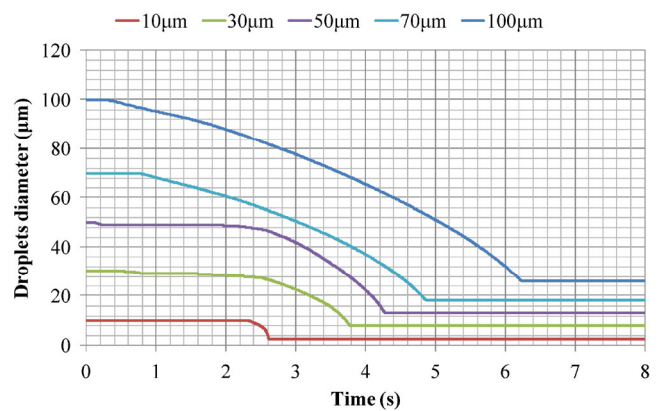

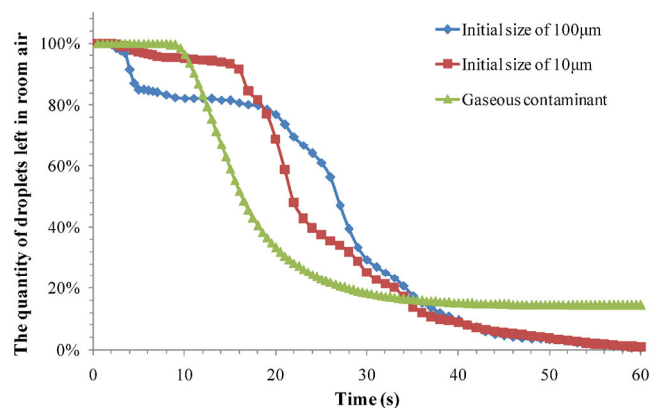**Fig. 7** The size change with time of the droplets with different initial sizes

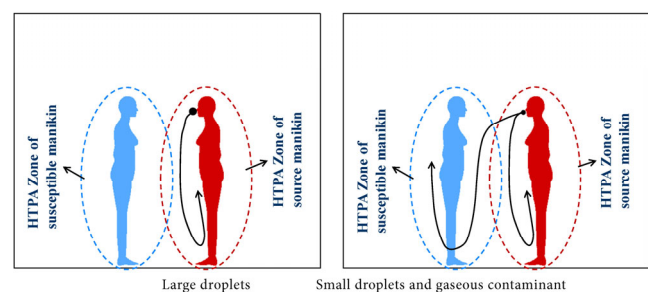**Fig. 8** The total quantity of droplets change with time in the UVPIR

Fig. 9 The schematic diagram of the dispersion process of the droplets in the UVPIR

jet to the HTPA zone of the susceptible manikin and lead to cross transmission. The remaining contaminants carried by the lower velocity coughing jet remain in the HTPA zone of the source manikin. This indicates that a potential effective measure to reduce person to person cross transmission in UVPIR is to decrease the velocity of coughing jet like wearing a mask.

4 Conclusions

We simulated the dispersion process of the droplets with initial diameter of 100 μm and 10 μm and gaseous contaminant in a UVPIR and studied the droplets dispersion characteristics and cross transmission with different sizes. We can get the following conclusions:

(1) For the droplets with initial size of 100 μm, the droplets settle out of the coughing jet quickly and cannot be carried by the coughing jet to the HTPA zone of the susceptible manikin. Almost all the droplets are left in the source manikin's HTPA zone and dispersion in it.

(2) The droplets with initial size of 10 μm and gaseous contaminant have similar dispersion process but different decay process in the UVPIR.

(3) Part of the small droplets and gaseous contaminant that are carried by the higher velocity coughing airflow can enter the HTPA zone of the susceptible manikin and disperse around it. The other part cannot spread to the susceptible manikin's HTPA zone and mainly spread in the source manikin's HTPA zone.

Acknowledgements

References

Arundel AV, Sterling EM, Biggin JH, Sterling TD (1986). Indirect health effects of relative humidity in indoor environments. *Environment Health Perspective*, 65: 351–361.

Barnes RA, Rogers TR (1989). Control of an outbreak of nosocomial aspergillosis by laminar air-flow isolation. *Journal of Hospital Infection*, 14: 89–94.

Brachman PS (1990). Transmission and principles of control. In: Mandell GL, Douglas RG, Bennett JE (eds), Principles and Practice of Infectious Diseases, 3rd edn. New York: Churchill Living Stone, pp. 155–158.

Cao G, Nielsen PV, Jensen RL, Heiselberg P, Liu L, Heikkinen J (2015). Protected zone ventilation and reduced personal exposure to airborne cross-infection. *Indoor Air*, 25: 307–319.

Chao CYH, Wan MP (2006). A study of the dispersion of expiratory aerosols in unidirectional downward and ceiling-return type airflows using a multiphase approach. *Indoor Air*, 16: 296–312.

Chao CYH, Wan MP, Morawska L, Johnson GR, Ristovski ZD, Hargreaves M, Mengersen K, Corbett S, Li Y, Xie X (2009). Characterization of expiration air jets and droplet size distributions immediately at the mouth opening. *Aerosol Science*, 40: 122–133.

Chen C, Zhao B, Cui W, Dong L, An N, Ouyang X (2010). The effectiveness of an air cleaner in controlling droplet/aerosol particle dispersion emitted from a patient's mouth in the indoor environment of dental clinics. *Journal of the Royal Society Interface*, 7: 1105–1118.

Chen F, Yu S, Lai A (2006). Modeling particle distribution and deposition in indoor environments with a new drift-flux model. *Atmospheric Environment*, 40: 357–367.

Clift R, Grace JR, Weber ME (1978). Bubbles, Drops, and Particles. New York: Academic Press.

Duguid JP (1946). The size and duration of air carriage of respiratory droplets and droplet nuclei. *Journal of Hygiene*, 44: 471–479.

FLUENT (2005). FLUENT Version 6.2. Fluent Inc.

Gastmeier P, Breier AC, Brandt C (2012). Influence of laminar airflow on prosthetic joint infections: A systematic review. *Journal of Hospital Infection*, 81: 73–78.

GB 50457-2008 (2009). Code for design of pharmaceutical industry clean room. Beijing: China Planning Press. (in Chinese)

Gregory FP, Marghi RM, Willianm TW (2007). Potential for airborne contamination in turbulent-and unidirectional-airflow compounding aseptic isolators. *American Journal of Health-System Pharmacy*, 64: 622–631.

Gupta JK, Lin CH, Chen Q (2009). Flow dynamics and characterization of a cough. *Indoor Air*, 19: 517–525.

Gupta JK, Lin CH, Chen Q (2010). Characterizing exhaled airflow from breathing and talking. *Indoor Air*, 20: 31–39.

Habchi C, Ghali K, Ghaddar N (2014). A simplified mathematical model for predicting cross contamination in displacement ventilation air-conditioned space. *Journal of Aerosol Science*, 76: 72–86.

Habchi C, Ghali K, Ghaddar N, Chakroun W, Alotaibi S (2016). Ceiling personalized ventilation combined with desk fans for reduced direct and indirect cross-contamination and efficient use of office space. *Energy Conversion and Management*, 111: 158–173.

He Q, Niu J, Gao N, Zhu T, Wu T (2011). CFD study of exhaled droplet transmission between occupants under different ventilation strategies in a typical office room. *Building and Environment*, 46: 397–408.

James M, Khan WS, Nannaparaju MR, Bhamra JS, Morgan-Jones R (2015). Current evidence for the use of laminar flow in reducing infection rates in total joint arthroplasty. *The Open Orthopaedics Journal*, 9: 495–498.

Li X, Niu J, Gao N (2011). Spatial distribution of human respiratory droplet residuals and exposure risk for the co-occupant under different ventilation methods. *HVAC&R Research*, 17: 432–445.

Li Y, Leung GM, Tang JW, Yang X, Chao CYH, Lin JZ, Lu JW, Nielsen PV, Niu J, Qian H (2007). Role of ventilation in airborne transmission of infectious agents in the built environment—A multidisciplinary systematic review. *Indoor Air*, 17: 2–18.

Lindsley WG, Blachere FM, Thewlis RE, Vishnu A, Davis KA, Cao G, Palmer JE, Clark KE, Fisher MA, Khakoo R (2010). Measurements of airborne influenza virus in aerosol particles from human coughs. *PLoS ONE*, 5(11): e15100.

McFadden ER, Pichurko BM, Bowman HF, Ingenito E, Burns S, Dowling N, Solway J (1985). Thermal mapping of the airways in humans. *Journal of Applied Physiology*, 58: 564–570.

McHugh SM, Hill ADK, Humphreys H (2015). Laminar airflow and the prevention of surgical site infection. More harm than good? *The Surgeon*, 13: 52–58.

Nielsen PV, Olmedo I, Ruiz de Adana M, Grzelecki P (2012). Airborne cross-infection risk between two people standing in surroundings with a vertical temperature gradient. *HVAC&R Research*, 18: 552–561.

Olmedo I, Nielsen PV, Ruiz de Adana M, Jensen RL (2013). The risk of airborne cross-infection in a room with vertical low-velocity ventilation. *Indoor Air*, 23: 62–73.

Passweg JR, Rowlings PA, Atkinson KA, Barrett AJ, Gale RP, Gratwohl A, Jacobsen N, Klein JP, Ljungman P, Russell JA, Schaefer UW, Sobocinski KA, Vossen JM, Zhang MJ, Horowitz MM (1998). Influence of protective isolation on outcome of allogeneic bone marrow transplantation for leukemia. *Bone Marrow Transplantation*, 21: 1231–1238.

Ranz WE, Marshall Jr WR (1952). Evaporation from drops, Part 2. *Chemical Engineering Progress*, 48: 173–180.

Riley RL (1974). Airborne infection. *The American Journal of Medicine*, 57: 466–475.

Schlesinger A, Paul M, Gafter-Gvili A, Rubinovitch B, Leibovici L (2009). Infection-control interventions for cancer patients after chemotherapy: A systematic review and meta-analysis. *The Lancet Infectious Diseases*, 9: 97–107.

Storb R, Prentice RL, Buckner CD, Clift RA, Appelbaum F, Deeg J, Doney K, Hansen JA, Mason M, Sanders JE, Singer J, Sullivan KM, Witherspoon, RP, Thomas ED (1983). Graft versus host disease and survival in patients with aplastic anaemia treated by marrow grafts from HLA-identical siblings-Beneficial effect of a protective environment. *The New England Journal of Medicine*, 308: 302–307.

Wells WF (1934). On air-borne infection study: II. Droplets and droplet nuclei. *American Journal of Epidemiology*, 20: 611–618.

Yang C, Yang X, Zhao B (2014). Person to person airborne particles cross transmission in vertical laminar air flow room. In: Proceedings of Indoor Air 2014, Hong Kong, China.

Yang C, Yang X, Zhao B (2015). The ventilation needed to control thermal plume and particle dispersion from manikins in a unidirectional ventilated protective isolation room. *Building Simulation*, 8: 551–565.

Yu ITS, Li Y, Wong TW, Tam W, Chan AT, Lee JHW, Leung DYC, Ho T (2004). Evidence of airborne transmission of the severe acute respiratory syndrome virus. *The New England Journal of Medicine*, 350: 1731–1739.

Zhao B, Wu J (2005). Numerical investigation of particle diffusion in a clean room. *Indoor and Built Environment*, 14: 469–479.

Zhao B, Zhang Y, Li X, Yang X, Huang DT (2004). Comparison of indoor aerosol particle concentration and deposition in different ventilated rooms by numerical method. *Building and Environment*, 39: 1–8.